

The oxygen isotope value of whole wood, α -cellulose, and holocellulose in modern and fossil wood

Junbo Ren^{a,b,c,*}, Brian A. Schubert^b, William E. Lukens^{d,**}, Chenxi Xu^c

^a College of Earth Sciences, Jilin University, Changchun 130061, China

^b School of Geosciences, University of Louisiana at Lafayette, Lafayette, LA 70504, USA

^c Key Laboratory of Cenozoic Geology and Environment, Institute of Geology and Geophysics, Chinese Academy of Sciences, Beijing 100029, China

^d Department of Geology and Environmental Science, James Madison University, Harrisonburg, VA 22807, USA

ARTICLE INFO

Editor: Michael E. Boettcher

Keywords:

Tree rings
Oxygen isotope
Cellulose extraction
Dendroclimate
Mummified wood

ABSTRACT

The oxygen isotope value ($\delta^{18}\text{O}$) of α -cellulose extracted from modern and fossil wood has been used widely to reconstruct climate throughout the Quaternary and deep-time. Substantial effort has been made towards developing more efficient and cost-effective methods for obtaining α -cellulose from whole wood, though some research groups advocate for measuring $\delta^{18}\text{O}$ directly on whole wood due to a constant offset between the $\delta^{18}\text{O}$ of whole wood and α -cellulose. The utility of alternative substrates to α -cellulose (e.g., whole wood or holocellulose) for paleoclimate reconstruction using fossil wood, however, has not been evaluated. Here we present 48 new $\delta^{18}\text{O}$ measurements on mummified (subfossil) wood ranging in age from Eocene to Miocene. Whereas the $\delta^{18}\text{O}$ value of whole wood and α -cellulose is only weakly related in these subfossils, there is a strong linear correlation between the $\delta^{18}\text{O}$ value of α -cellulose and holocellulose. We augmented this dataset with 1546 new and published oxygen isotope pairs on whole wood, α -cellulose, and holocellulose from modern wood (Quaternary to present) to compare with our pre-Quaternary fossil samples. In contrast to the fossil wood, we found strong correlations between α -cellulose and whole wood and α -cellulose and holocellulose in modern samples. This finding suggests that all three substrates (whole wood, cellulose and holocellulose) derive oxygen isotopes from a common source (i.e., meteoric water) on a global scale, and that processing of α -cellulose may not be required for modern wood in some settings. Because average holocellulose yields in fossil wood were approximately double that of α -cellulose ($22.2 \pm 12.8\%$ versus $11.6 \pm 10.3\%$), $\delta^{18}\text{O}$ analysis on holocellulose rather than α -cellulose should produce reliable environmental data while reducing time and sample material required.

1. Introduction

Oxygen isotope of tree-ring α -cellulose ($\delta^{18}\text{O}_{\alpha\text{-cel}}$) is mainly controlled by the $\delta^{18}\text{O}$ of source water (commonly regarded as meteoric water, $\delta^{18}\text{O}_{\text{MW}}$), the relative humidity (RH) and post-photosynthesis process (Gessler et al., 2014; Miranda et al., 2021; Roden et al., 2000). Post-photosynthetic processes have little impact on $\delta^{18}\text{O}_{\alpha\text{-cel}}$, thereby providing a useful substrate for paleoclimate reconstruction (Jahren and Sternberg, 2003; Managave et al., 2020). In modern settings, the relative contribution to $\delta^{18}\text{O}_{\alpha\text{-cel}}$ from $\delta^{18}\text{O}$ of source water and RH depends on time scales and locations. For example, RH may play a more important role on regulating $\delta^{18}\text{O}_{\alpha\text{-cel}}$ in xeric environments than $\delta^{18}\text{O}_{\text{MW}}$ (Xu et al., 2021), while $\delta^{18}\text{O}_{\text{MW}}$ can dominate seasonal $\delta^{18}\text{O}_{\alpha\text{-cel}}$ variations in

humid environments (Baker et al., 2016).

Combining oxygen isotope and hydrogen isotope of fossil wood, RH and $\delta^{18}\text{O}_{\text{MW}}$ can be reconstructed (Jahren and Sternberg, 2003). Despite some uncertainties, $\delta^{18}\text{O}_{\alpha\text{-cel}}$ can be used as a proxy for $\delta^{18}\text{O}_{\text{MW}}$ in deep time (Rees-Owen et al., 2021; Ren et al., 2021; Richter et al., 2008b). Since oxygen isotopes behave differently between biomolecular substrates (e.g., resin, lignin, holocellulose, hemicellulose, and α -cellulose) within wood tissue (Barbour et al., 2001; Cullen and MacFarlane, 2005; Zech et al., 2014), chemical extraction of α -cellulose from living trees and fossil wood is therefore an important tool for quantifying past climate beyond the instrumental record (Ballantyne et al., 2006; Csank et al., 2013; Jahren and Sternberg, 2003; Rees-Owen et al., 2021; Ren et al., 2021; Richter et al., 2008a; Schubert and Jahren, 2015; Xu et al.,

* Corresponding author at: College of Earth Sciences, Jilin University, Changchun 130061, China.

** Corresponding author.

E-mail addresses: renjb18@mails.jlu.edu.cn (J. Ren), lukenswe@jmu.edu (W.E. Lukens).

2018).

Multiple methods have been developed for the chemical extraction and purification of α -cellulose from tree rings (Brendel et al., 2000; Green, 1963; Leavitt and Danzer, 1993; Sauer and Sternberg, 1994). Because these methods all increase the time, cost, and sample size required for analysis, researchers have developed methods to improve efficiency, reduce sample loss, and optimize high-throughput sampling (Andreu-Hayles et al., 2019; Greer et al., 2018; Hook et al., 2015; Kagawa et al., 2015; Li et al., 2011; Loader et al., 2015; Wieloch et al., 2011; Xu et al., 2011). Nonetheless, other studies have shown a close correspondence between the $\delta^{18}\text{O}$ value of whole wood ($\delta^{18}\text{O}_{\text{wood}}$) and $\delta^{18}\text{O}_{\alpha\text{-cel}}$, which suggests that the time and resources expended in cellulose extraction may be unnecessary to reconstruct $\delta^{18}\text{O}_{\text{MW}}$ value (Barbour et al., 2001; Borella et al., 1999; Gori et al., 2013; Guerrieri et al., 2017; Nakai et al., 2018; Pons and Helle, 2011; Sidorova et al., 2010). A limited number of studies have also investigated holocellulose, which is comprised of both α -cellulose and hemicellulose and does not require treatment with NaOH, as an alternative to purified α -cellulose (Cullen and MacFarlane, 2005; Ferrio and Voltas, 2005; Szymczak et al., 2011; Voltas et al., 2008; Wright, 2008). A lack of consensus contributes doubt over whether $\delta^{18}\text{O}_{\text{wood}}$ can be used as a reliable recorder of $\delta^{18}\text{O}_{\text{MW}}$ value. Yet, all of the above studies investigated living or recently felled trees unaffected by diagenesis and cellulose degradation. In contrast to these unaltered samples, fossil wood may contain little to no α -cellulose (Lukens et al., 2019); therefore, analysis of whole wood might open new analytical opportunities for reconstructing climate in deep time using wood of various preservation states.

Our previous work showed that the stable carbon isotopic composition of whole wood ($\delta^{13}\text{C}_{\text{wood}}$) correlated strongly with the carbon isotope value of α -cellulose ($\delta^{13}\text{C}_{\alpha\text{-cel}}$) within both modern and fossil samples (Lukens et al., 2019), suggesting extraction of α -cellulose was not necessary when patterns of $\delta^{13}\text{C}$ data are used in proxy system models (e.g., Vornlocher et al., 2021). These prior analyses also revealed that a larger apparent enrichment exists between $\delta^{13}\text{C}_{\alpha\text{-cel}}$ and $\delta^{13}\text{C}_{\text{wood}}$ in deep-time samples relative to modern trees, which demonstrates a need for correcting deep-time $\delta^{13}\text{C}_{\text{wood}}$ data where $\delta^{13}\text{C}_{\alpha\text{-cel}}$ analysis is

untenable. However, the fidelity of $\delta^{18}\text{O}$ signals across compounds in modern and fossil wood may differ from that of $\delta^{13}\text{C}$ for several reasons. Tree ring $\delta^{18}\text{O}$ values can be influenced by post-photosynthetic reactions that can involve the exchange of oxygen isotopes, including the use of xylem water during cellulose formation, exchange with organics during phloem transport, and exchange with intracellular water during lignin biosynthesis (Gessler et al., 2009; Gessler et al., 2014; Song et al., 2022). Variable preservation potential of cellulose, lignin, and extractives may affect the apparent enrichment of oxygen isotopes between whole wood and cellulose.

Here, we report new measurements on $\delta^{18}\text{O}_{\alpha\text{-cel}}$ and $\delta^{18}\text{O}_{\text{wood}}$ within modern (Holocene to present) and fossil (pre-Quaternary) wood samples that represent a wide range of preservation states (1.2% to 43% α -cellulose) in order to test the efficacy of $\delta^{18}\text{O}_{\text{wood}}$ as a reliable substitute for $\delta^{18}\text{O}_{\alpha\text{-cel}}$ in modern and fossil wood. We further investigate the potential for $\delta^{18}\text{O}$ value of holocellulose ($\delta^{18}\text{O}_{\text{h-cel}}$) to be a reliable alternative to determination of $\delta^{18}\text{O}_{\alpha\text{-cel}}$ in the fossil record.

2. Materials and methods

To obtain a broad spatial and temporal coverage of tree ring $\delta^{18}\text{O}$ values under wide-ranging environmental conditions, 16 fossil deep-time samples and 6 Holocene wood samples were analyzed for this study (Fig. 1). Deep-time specimens included: 1) four Eocene samples collected from Banks Island, Canada; 2) five Oligocene samples collected from Nanning basin, China; and 3) seven Miocene samples collected from northeastern Siberia (Finish Stream site near Cherskiy, Russia, Schubert et al., 2017) and multiple sites across China. Holocene samples included: 1) one ~2000-year-old *Cupressus* sp. collected from sediments near New Orleans, Louisiana, USA; 2) one ~3000-year-old sample collected from permafrost sediments at Duvanny Yar, Sakha Republic, Russia; 3) one ~200-year-old *Pinus* sp. collected from the Roy House, Lafayette, Louisiana, USA. Sample site locations and descriptions are shown in the Table 1, and more details are provided in Supplement.

Subsamples of whole wood from each of the 22 samples were homogenized to a powder (< 0.1 mm) using a ball mill (Spex 8000 Mixer/

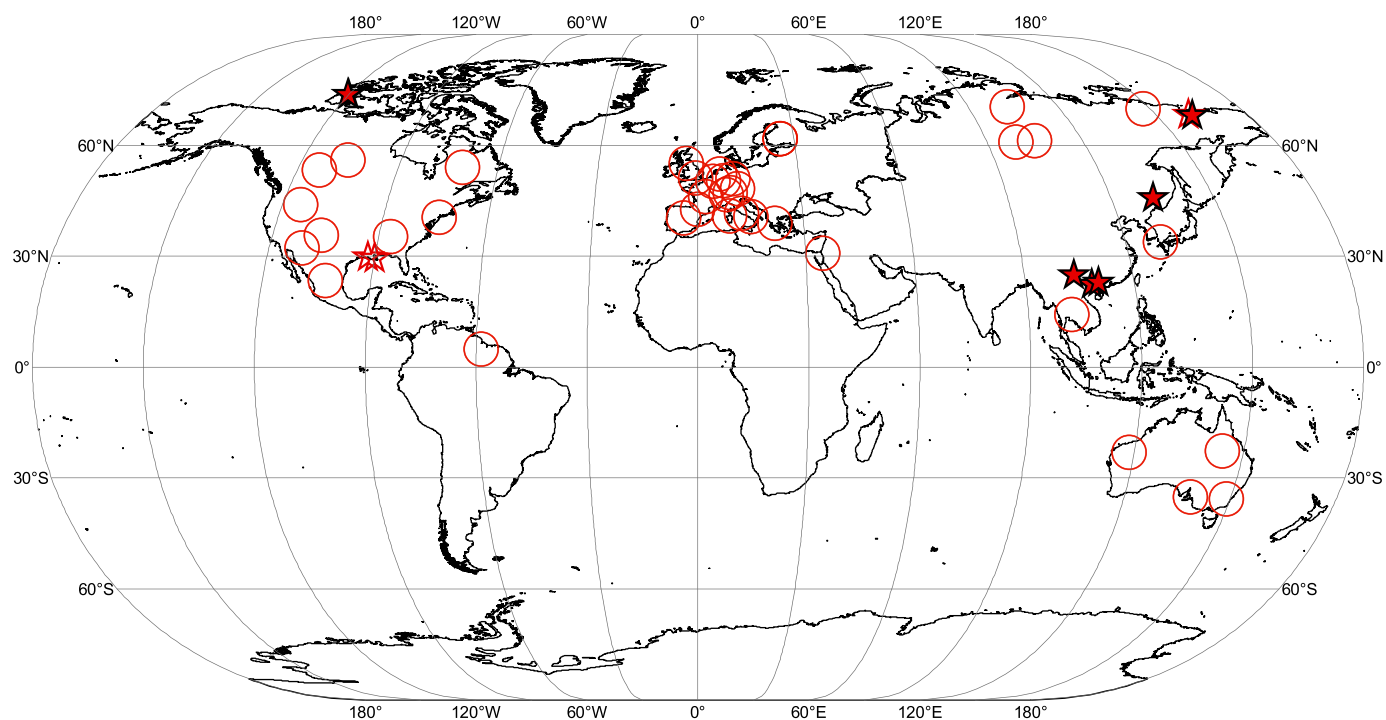


Fig. 1. Map showing locations of new (stars) and published (circles) oxygen isotope data analyzed for this study (see details in the Supplement). Open symbols indicate modern samples, and filled symbols indicate deep-time (pre-Quaternary) fossil samples.

Table 1

The list of samples in this study.

Location	Age interval	No. of samples
Banks Island, Canada	Eocene	4
Nanning Basin, China	Oligocene	5
Cherskiy, Russia	Miocene	1
Baoqing, China	Miocene	2
Guiping Basin, China	Miocene	2
Qujing, China	Miocene	2
Duvanny Yar, Russia	Holocene (3 ka)	2
New Orleans, USA	Holocene (2 ka)	1
Lafayette, USA	Holocene (0.2 ka)	3

Note: All samples consisted of bulk wood averaged across ~2–3 rings. The sample from Lafayette, USA, consists of subsamples across the upper, middle and bottom sections of a timber from the Roy House.

Mill, USA) with stainless steel vial and ball, and then divided into three approximately equal aliquots. Approximately one-third of each aliquot was set aside for analysis of $\delta^{18}\text{O}_{\text{wood}}$, while the remaining material was split between two 1.5 ml polyethylene microcentrifuge tubes and designated for cellulose extraction (α -cellulose and holocellulose, respectively) using the modified Brendel method (Brendel et al., 2000; Gaudinski et al., 2005). Lignin and non-cellulose polysaccharides were first removed from each sample by adding a 10:1 ratio of 80% acetic acid to 70% nitric acid (i.e., 360 μl 80% acetic acid and 36 μl 70% nitric acid), gently mixing, and then heating in an aluminum heating-block at 120 °C for 30 min. Samples were allowed to cool for 5 to 10 min and the resulting material, comprised of holocellulose, was then washed twice in 1 ml of 99% ethanol, and then once each in 1 ml of DI water, 300 μl of 99% ethanol, and finally 300 μl of acetone. Samples were then dried overnight at 50 °C. One aliquot was then set aside for analysis of holocellulose, while the other aliquot was washed in an additional step for 10 min in 300 μl of NaOH (17% w/v) to isolate α -cellulose then again rinsed in the following: 1) 1 ml of DI water, 2) 260 μl of DI water and 36 μl of 80% acetic acid, 3) 1 ml of DI water, 4) 300 μl of 99% ethanol, 5) 300 μl of acetone, before being again dried overnight at 50 °C. All the above steps were completed in triplicate so that for each wood sample, we recovered three different replicate subsamples of whole wood, holocellulose, and α -cellulose for stable isotope analysis.

The dried whole wood, holocellulose, and α -cellulose were then weighed into silver capsules, and $\delta^{18}\text{O}$ values were determined using a High-Temperature-Conversion Elemental Analyzer coupled with a Delta-V Advantage Mass Spectrometer (Thermo Fisher Scientific, Inc., USA) at the University of Louisiana at Lafayette. Samples were analyzed with three internal laboratory reference materials (ACELL = 32.33 \pm 0.06‰, JCELL01 = 17.64 \pm 0.09‰, and SigmaCell = 28.46 \pm 0.07‰) calibrated against International Atomic Energy Agency (IAEA) benzoic acid reference materials: IAEA 601 (23.24 \pm 0.19‰) and IAEA 602 (71.28 \pm 0.36‰). A quality assurance sample (JCELL02, $\delta^{18}\text{O}$ = 20.44 \pm 0.10‰) was analyzed within each batch and analyzed as an unknown. The analytical precision of the quality assurance sample was 0.2‰ (1 σ , n = 12). The $\delta^{18}\text{O}$ values are reported as the average of three replicate samples relative to the VSMOW standard.

We quantified isotopic differences between substrates by calculating offsets in $\delta^{18}\text{O}$ value between substrates [ϵ , or apparent enrichment, after (Craig, 1954)] after averaging $\delta^{18}\text{O}$ values of replicate samples, where:

$$\epsilon_{\text{O}} = \delta^{18}\text{O}_{\alpha\text{-cel}} - \delta^{18}\text{O}_{\text{wood}} \quad (1)$$

$$\epsilon'_{\text{O}} = \delta^{18}\text{O}_{\text{h-cel}} - \delta^{18}\text{O}_{\text{wood}} \quad (2)$$

In all cases, simple subtraction of $\delta^{18}\text{O}$ values between substrates yielded offset estimates that were within analytical uncertainty (i.e., \leq 0.2‰) of other approaches to calculating apparent enrichment, for example:

$$\epsilon = \left[\left(\delta^{18}\text{O}_{\alpha\text{-cel}} + 1000 \right) / \left(\delta^{18}\text{O}_{\text{wood}} + 1000 \right) - 1 \right] \quad (3)$$

3. Statistical methods

Statistical analyses and visualizations were performed in RStudio 4.2.2 (R Core Team, 2022) using the following packages: gghalves (Tiedemann, 2022); here (Müller, 2020); and tidyverse (Wickham et al., 2019). Differences in $\delta^{18}\text{O}$ value measured on whole wood, holocellulose, and α -cellulose were assessed by binning data by geologic epoch, given that ice volume and global temperature—and therefore $\delta^{18}\text{O}_{\text{MW}}$ —change over such timespans (Westerhold et al., 2020). Within each time bin, a non-parametric Kruskal-Wallis test was performed with substrate (whole wood, holocellulose, and α -cellulose) as a grouping variable and $\delta^{18}\text{O}$ value as the outcome. This approach was chosen due to deviations from normality, which were first assessed using the Shapiro-Wilk test at the 0.05 significance level. In cases where the Kruskal-Wallis test indicated significant differences between groups, Dunn's test was performed post hoc to assess directionality in differences of mean ranks. Bonferroni adjustments were made for p -values in the multiple comparisons test.

Differences in the yield of holocellulose and α -cellulose from individual specimens of fossil and modern wood analyzed in this study were assessed using the Wilcoxon signed rank-sum test, as groups of data deviated from normality and the samples are paired between extraction protocols. Here, cellulose extraction protocol was assigned as the grouping variable and cellulose yield as the outcome.

We applied the Wilcoxon rank-sum test to test for differences in median values of $\delta^{18}\text{O}$ offset (ϵ_{O} and ϵ'_{O}) between fossil (deep-time) versus modern (Holocene) wood. This non-parametric test was chosen because preliminary analyses using the Shapiro-Wilk test found data distributions that deviated from normality and samples were not paired.

Finally, linear regression was used in assessing the association and spread of $\delta^{18}\text{O}$ values across substrates. The significance level for all tests was set at 0.05. These approaches were applied only on data sets that had numbers of observations sufficient to provide meaningful results; otherwise, qualitative comparisons between data groups were made. All data sets are available in the Supplementary Materials.

4. Results and discussion

Stable isotope analyses of the fossil (n = 16) and modern (n = 6) samples yielded a wide range of $\delta^{18}\text{O}_{\alpha\text{-cel}}$, $\delta^{18}\text{O}_{\text{h-cel}}$, and $\delta^{18}\text{O}_{\text{wood}}$ values (Table 2), consistent with the wide range of environments from which these specimens are sourced (Fig. 2A). For each time bin, $\delta^{18}\text{O}_{\text{wood}}$ differed significantly from $\delta^{18}\text{O}_{\alpha\text{-cel}}$ and $\delta^{18}\text{O}_{\text{h-cel}}$ measured on the same specimen (Kruskal-Wallis followed by Dunn's test, p < 0.05; Fig. 2A). However, $\delta^{18}\text{O}_{\alpha\text{-cel}}$ and $\delta^{18}\text{O}_{\text{h-cel}}$ on paired samples were not significantly different on average ($p \geq 0.05$).

Yields of α -cellulose (based on weight) within the fossil samples ranged from 1.2 to 42.8% (Fig. 2B), consistent with the wide range of preservation states represented by our samples (Lukens et al., 2019).

Table 2Summary of new $\delta^{18}\text{O}$ analyses from fossil and modern wood.

Substrate	Fossil (Deep-time)				Modern (Holocene)			
	Mean	sd	Range	n	Mean	sd	Range	n
$\delta^{18}\text{O}_{\alpha\text{-cel}}$ (‰)	22.0	2.1	8.0	16	26.2	7.6	15.9	6
$\delta^{18}\text{O}_{\text{h-cel}}$ (‰)	22.5	1.9	7.5	16	26.5	7.2	15.2	6
$\delta^{18}\text{O}_{\text{wood}}$ (‰)	15.6	2.9	15.6	16	20.7	7.1	9.5	6

Note: Abbreviations are as follows: sd = standard deviation, range = the difference between the maximum value and the minimum value for each substrate ($\delta^{18}\text{O}_{\text{max}} - \delta^{18}\text{O}_{\text{min}}$), n = number of samples in group. Deep-time samples include Eocene, Oligocene, and Miocene epochs (i.e., pre-Quaternary). Raw data is presented in the Supplement.

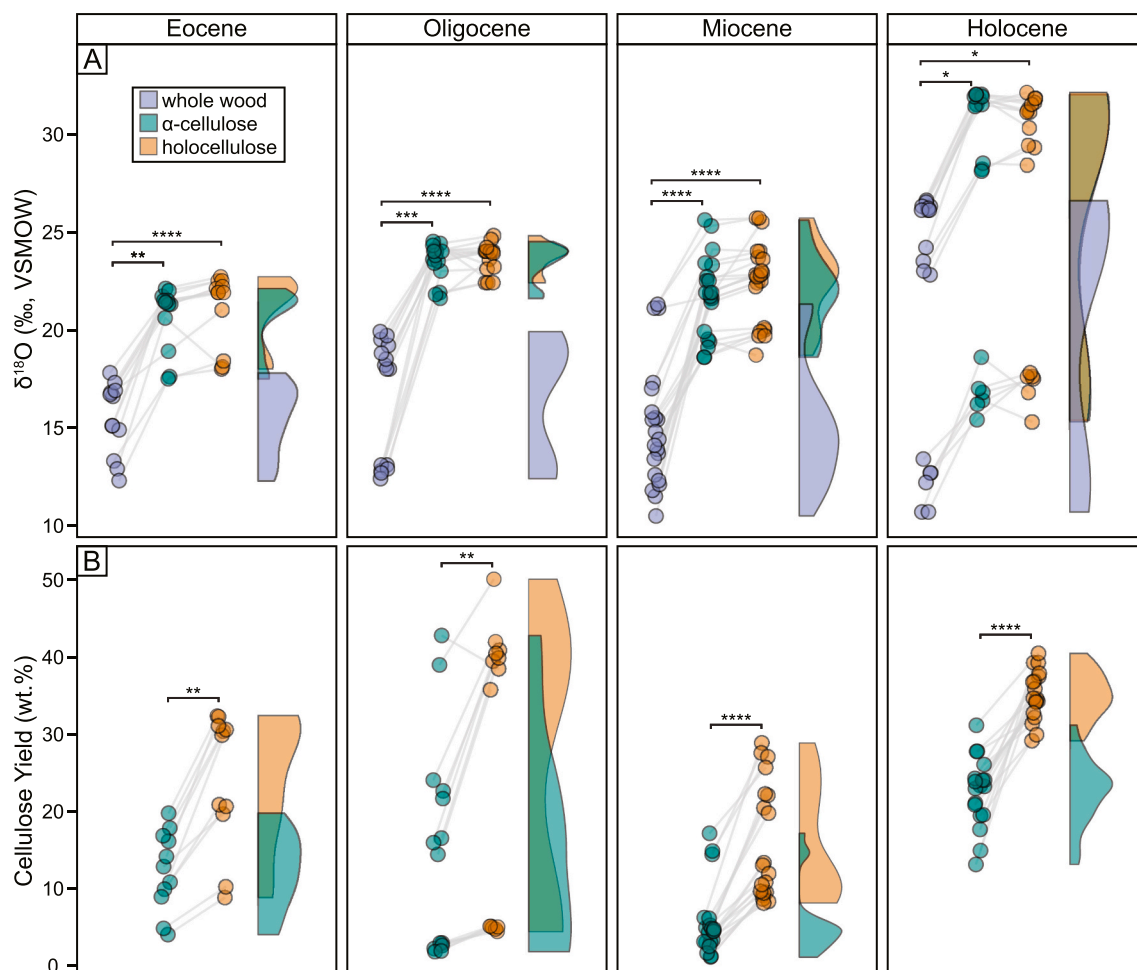


Fig. 2. Raincloud plots (kernel density functions with data points) of the A) $\delta^{18}\text{O}$ value ($n = 198$) and B) cellulose yield ($n = 126$) for samples analyzed in this study. Sample substrates are color coded according to legend in first box of panel A. Gray lines connect aliquots across substrates; all data from replicate analyses are shown as individual points ($n = 198$). Brackets indicate significant differences between groups from statistical tests (panel A: Dunn's test; panel B: Wilcoxon signed rank sum test; see Methods), where: * = $p < 0.05$; ** = $p < 0.005$; *** = $p < 0.0005$; **** = $p < 0.00005$. Pairs without brackets were not significantly different. (For interpretation of the references to color in this figure legend, the reader is referred to the web version of this article.)

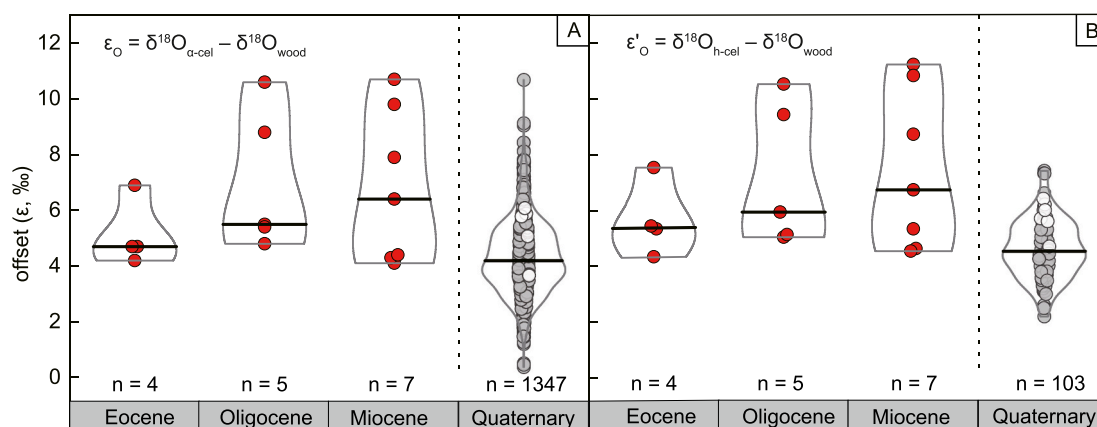


Fig. 3. Violin plots of offset between $\delta^{18}\text{O}_{\text{wood}}$ and $\delta^{18}\text{O}_{\alpha\text{-cel}}$ (i.e., ϵ_o , Eq. (1)) (A) and $\delta^{18}\text{O}_{\text{wood}}$ and $\delta^{18}\text{O}_{\text{h-cel}}$ (i.e., ϵ'_o , Eq. (2)) (B) in different geological time slices. Red circles and white symbols indicate fossil and Holocene wood (respectively) analyzed in this study. Gray symbols indicate data compiled from the literature. The Quaternary time bin includes both Holocene and Pleistocene samples. Each “violin” represents the probability distribution of ϵ values in each group normalized to the same area, with cross-bar indicating median value. (For interpretation of the references to color in this figure legend, the reader is referred to the web version of this article.)

Cellulose yields differed significantly for paired samples in four time bins (Wilcoxon signed rank sum test, $p < 0.05$; Fig. 2B). In each group, holocellulose extraction produced larger yields than α -cellulose on average. Out of the 62 paired extractions, we note that only one sample (NNW069–01) produced lower holocellulose than α -cellulose, which may have been due to sample loss during laboratory preparation.

The range in $\delta^{18}\text{O}$ values reported here (Fig. 2, Table 2) is larger than observed for previous studies comparing oxygen isotope values of cellulose and whole wood (Sternberg et al., 2007; Xu et al., 2021), but still only represents approximately half the range of $\delta^{18}\text{O}$ values reported for trees growing across the planet today (Ren et al., 2021). We therefore augmented our dataset with paired $\delta^{18}\text{O}_{\alpha\text{-cel}}\text{-}\delta^{18}\text{O}_{\text{wood}}$, $\delta^{18}\text{O}_{\alpha\text{-cel}}\text{-}\delta^{18}\text{O}_{\text{h-cel}}$, and $\delta^{18}\text{O}_{\text{h-cel}}\text{-}\delta^{18}\text{O}_{\text{wood}}$ values from 24 published studies, yielding a total of 3320 stable isotope measurements and 1546 pairs (1363 $\delta^{18}\text{O}_{\alpha\text{-cel}}$ and $\delta^{18}\text{O}_{\text{wood}}$ pairs, 64 $\delta^{18}\text{O}_{\alpha\text{-cel}}$ and $\delta^{18}\text{O}_{\text{h-cel}}$ pairs, and 119 $\delta^{18}\text{O}_{\text{h-cel}}$ and $\delta^{18}\text{O}_{\text{wood}}$ pairs; Supplement). This comprehensive dataset of new and published $\delta^{18}\text{O}$ values includes data from both field and herbarium collections and at least 54 genera sampled across 53 degrees of latitude. In order to compare the effect of diagenesis on oxygen isotope value, we separated the dataset into two age categories: modern (Quaternary to present, $n = 3179$) and deep-time (pre-Quaternary, $n = 141$).

We observed a wide range of ϵ_{O} values for fossil samples (ϵ_{O} : 4.1–10.7‰) that tend to be higher on average (Wilcoxon rank-sum test, $p < 0.001$) but overlap in value with modern samples (ϵ_{O} : 0.4–10.7‰) (Fig. 3A). Likewise, ϵ'_{O} values from fossils (ϵ'_{O} : 4.3–11.2‰) are greater on average (Wilcoxon rank-sum test, $p < 0.001$) compared to modern samples (ϵ'_{O} : 2.2–8.4‰), and fossil ϵ'_{O} values extend to higher values that are not observed in the modern specimens (Fig. 3B). This latter observation may be due to under-sampling of modern $\delta^{18}\text{O}_{\text{h-cel}}$ space. Although each of the deep-time age bins contain too few samples to analyze quantitatively, we do not observe any evidence for systematic $\delta^{18}\text{O}$ offset through time in the pre-Quaternary samples. Variability between deep-time sample $\delta^{18}\text{O}$ offset values is best attributed to variable preservation state between individual fossil assemblages rather than long-term temporal control on wood decay.

Previous studies of modern wood have reported a wide range of

relationships between $\delta^{18}\text{O}_{\alpha\text{-cel}}$ and $\delta^{18}\text{O}_{\text{wood}}$ (e.g., Ferrio and Voltas, 2005; Gori et al., 2013; Guerrieri et al., 2017; Szymczak et al., 2011) (Supplement). The slope of many of these relationships deviates significantly from 1 (range = 0.18 to 1.29), suggesting a non-uniform offset between $\delta^{18}\text{O}_{\alpha\text{-cel}}$ and $\delta^{18}\text{O}_{\text{wood}}$. The range of $\delta^{18}\text{O}$ values investigated within each study, however, was small compared to the more comprehensive data set in the current investigation; our new compilation allows for a more complete assessment of global relationships between $\delta^{18}\text{O}$ among the three commonly measured substrates in wood tissue.

Analysis of the full range of $\delta^{18}\text{O}$ values represented by our global compilation reveals a strong linear relationship between $\delta^{18}\text{O}_{\text{wood}}$ and $\delta^{18}\text{O}_{\alpha\text{-cel}}$ for the modern samples ($R^2 = 0.94$, $n = 1347$; Fig. 4A) across diverse species and environments. However, the slope and its associated standard error ($m = 1.12 \pm 0.01$) of this relationship deviates from unity, indicating a larger offset between $\delta^{18}\text{O}_{\text{wood}}$ and $\delta^{18}\text{O}_{\alpha\text{-cel}}$ (ϵ_{O}) in settings with higher $\delta^{18}\text{O}$. We hypothesize that this deviation from unity is caused by variability in wood tissue composition across trees on a global scale. For example, trees living in humid, low-latitude sites tend to produce copious amounts of oils and resin, which carry low $\delta^{18}\text{O}$ values and would therefore decrease bulk $\delta^{18}\text{O}_{\text{wood}}$ values without affecting $\delta^{18}\text{O}_{\alpha\text{-cel}}$ (Barbour et al., 2001; Cullen and MacFarlane, 2005; Langenheim, 1990; Nissenbaum et al., 2005). Alternatively, the deviation from a 1:1 relationship between $\delta^{18}\text{O}_{\text{wood}}$ and $\delta^{18}\text{O}_{\alpha\text{-cel}}$ could be due to a sampling bias against high-latitude/altitude or colder settings that contain low $\delta^{18}\text{O}_{\text{wood}}$ and $\delta^{18}\text{O}_{\alpha\text{-cel}}$ values (e.g., Dansgaard, 1964). Further work is needed to test this hypothesis.

In contrast to modern samples, a much weaker relationship was observed between $\delta^{18}\text{O}_{\alpha\text{-cel}}$ and $\delta^{18}\text{O}_{\text{wood}}$ for the fossils we analyzed ($R^2 = 0.21$, $n = 46$; Fig. 4A). Thus, determination of $\delta^{18}\text{O}_{\text{wood}}$ might represent an alternative to $\delta^{18}\text{O}_{\alpha\text{-cel}}$ from living and recently felled trees, but isotopic exchange and cellulose loss during diagenesis mean that $\delta^{18}\text{O}_{\text{wood}}$ has limited utility for quantifying environmental change from fossil samples. Lignin has a much lower $\delta^{18}\text{O}$ value compared to cellulose extracted from the same wood tissue ($\sim 10\%$; Barbour et al., 2001; Gray and Thompson, 1977). Therefore, progressive cellulose loss during diagenesis would lower $\delta^{18}\text{O}_{\text{wood}}$ and may be one pathway for

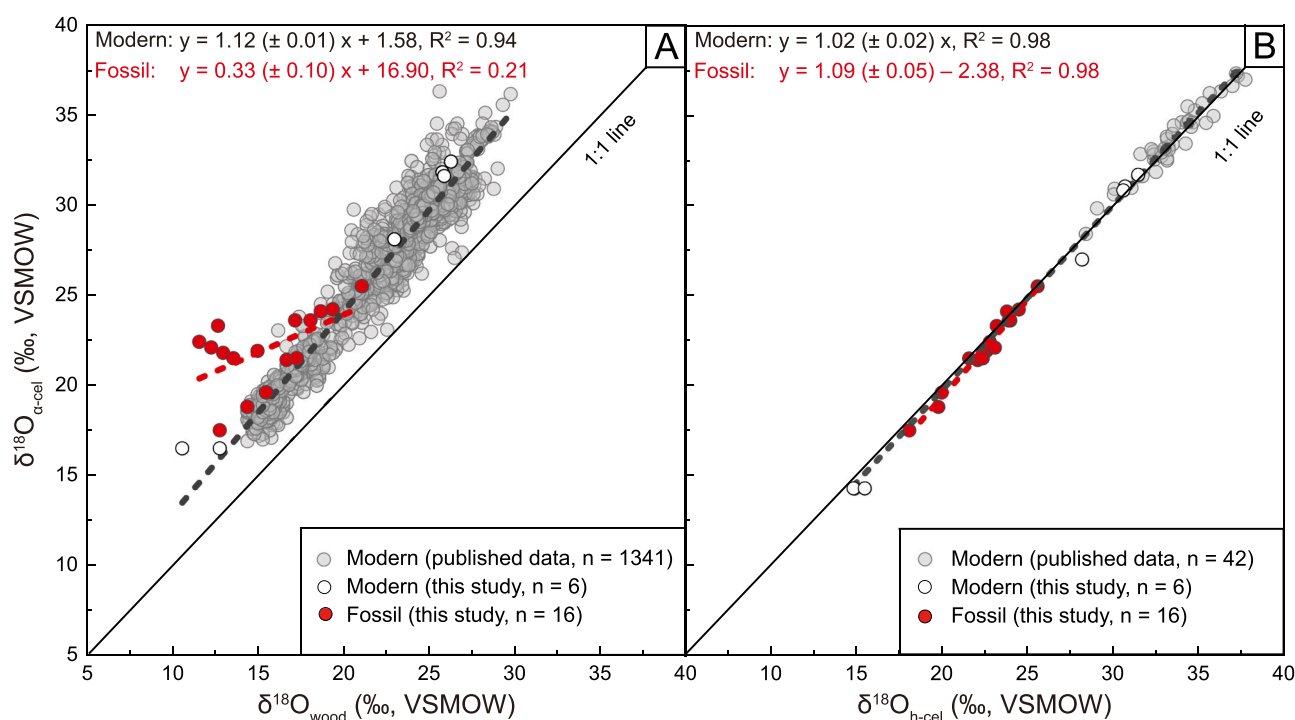


Fig. 4. Cross-plot of $\delta^{18}\text{O}_{\text{wood}}$ versus $\delta^{18}\text{O}_{\alpha\text{-cel}}$ (a) and $\delta^{18}\text{O}_{\text{h-cel}}$ versus $\delta^{18}\text{O}_{\alpha\text{-cel}}$ (b) for modern and fossil wood. Deviation from 1:1 line indicates offset (ϵ) between $\delta^{18}\text{O}_{\alpha\text{-cel}}\text{-}\delta^{18}\text{O}_{\text{wood}}$ and $\delta^{18}\text{O}_{\alpha\text{-cel}}\text{-}\delta^{18}\text{O}_{\text{h-cel}}$. Coefficient of determination (R^2) and slope (\pm standard error) are shown for each linear regression model.

generation of higher ϵ_{O} and ϵ'_{O} values in wood fossils.

Our new analyses combined with published $\delta^{18}\text{O}_{\text{h-cel}}$ and $\delta^{18}\text{O}_{\alpha\text{-cel}}$ pairs showed these two substrates to have a strong linear relationship for both modern ($R^2 = 0.98$, $n = 47$) and deep-time samples ($R^2 = 0.98$, $n = 16$) (Fig. 4B). The strong coefficients of determination and slopes that are near unity (modern: $m = 1.02 \pm 0.02$; fossil: $m = 1.09 \pm 0.05$) indicate that coherent $\delta^{18}\text{O}$ data are recorded across α -cellulose and holocellulose, regardless of the diagenetic history of a wood specimen. Similar agreement between $\delta^{18}\text{O}_{\alpha\text{-cel}}$ and $\delta^{18}\text{O}_{\text{h-cel}}$ has been observed previously for modern samples across a smaller range of $\delta^{18}\text{O}$ values (Cullen and MacFarlane, 2005; Wright, 2008). The larger compilation of the current study shows this association is robust across a wide range of species and environments, and includes the first comparison within deep-time samples. The potential for holocellulose to serve as an alternative substrate to α -cellulose is particularly promising for deep-time fossils, which may have limited sample size and only small quantities of preserved α -cellulose. Because yields of holocellulose (mean = $22.2 \pm 12.8\%$) are $\sim 2\times$ greater than for α -cellulose on average (mean = $11.6 \pm 10.3\%$) in fossil samples (Fig. 2B), determination of $\delta^{18}\text{O}_{\text{h-cel}}$ rather than $\delta^{18}\text{O}_{\alpha\text{-cel}}$ may open new possibilities for higher-resolution analysis and less sample destruction of small or irreplaceable fossil samples.

5. Conclusion

Chemical separation and purification of α -cellulose from whole wood have become standard practice for generating robust tree-ring oxygen isotope data (e.g., McCarroll and Loader, 2004). Here, we demonstrated that whole wood $\delta^{18}\text{O}$ values can be used in lieu of the α -cellulose for interpretation of $\delta^{18}\text{O}$ trends in modern wood, but differences between $\delta^{18}\text{O}_{\alpha\text{-cel}}$ and $\delta^{18}\text{O}_{\text{wood}}$ values were not constant. Thus, no single correction factor can be applied to $\delta^{18}\text{O}_{\text{wood}}$ data from fossil wood to relate them to $\delta^{18}\text{O}_{\alpha\text{-cel}}$ data, and therefore to $\delta^{18}\text{O}_{\text{MW}}$. This suggests chemical extraction of cellulose extraction is necessary for accurate interpretation of $\delta^{18}\text{O}$ values but that the robust correlation between $\delta^{18}\text{O}_{\alpha\text{-cel}}$ and $\delta^{18}\text{O}_{\text{wood}}$ values in living trees does not necessitate cellulose extraction unless variations in $\delta^{18}\text{O}$ values are very low in the data sets under study (Helle et al., 2022).

In contrast, examination of fossil, pre-Quaternary wood samples did not yield a significant relationship between $\delta^{18}\text{O}_{\alpha\text{-cel}}$ and $\delta^{18}\text{O}_{\text{wood}}$, suggesting diagenesis affects the $\delta^{18}\text{O}$ value of whole wood on geologic timescales. However, we identified for the first time, a 1:1 relationship between the $\delta^{18}\text{O}$ value of holocellulose and α -cellulose in fossil wood. We note that analysis of holocellulose is beneficial over α -cellulose because it allows for analysis of more degraded fossil samples with a lower preserved cellulose content, and higher resolution sampling due to the smaller amount of starting material required for analysis of $\delta^{18}\text{O}_{\text{h-cel}}$ versus $\delta^{18}\text{O}_{\alpha\text{-cel}}$. Together this comparison of $\delta^{18}\text{O}_{\text{wood}}$, $\delta^{18}\text{O}_{\alpha\text{-cel}}$, and $\delta^{18}\text{O}_{\text{h-cel}}$ across wood of various ages and states of degradation is promising for the development of longer and higher-resolution records of $\delta^{18}\text{O}$ trends using modern [including archaeological wood suffered aging and decay (Domínguez-Delmás, 2020)] and fossil wood.

Declaration of Competing Interest

The authors declare that they have no known competing financial interests or personal relationships that could have appeared to influence the work reported in this paper.

Data availability

I have shared my data at the Attach File step

Acknowledgments

This work was supported by National Science Foundation grant no. AGS-1903601. We thank Yingfeng Xu for laboratory assistance, and Tom

Doyle, Geoffrey Thompson, and Cheng Quan for providing wood samples: Doyle-01 (Doyle), Roy01, Roy02, and Roy03 (Thompson), and NNW015, NNW024, NNW065, NNW069, NNW073, BQ-02, BQ-05, GPW013, GPW062, YNW02, YNW05 (Quan). Samples from Aulavik National Park on northern Banks Island, Northwest Territories, Canada, were collected by Schubert in July 2012 on a field expedition led by Jaelyn Eberle (University of Colorado at Boulder, USA), which was financially supported by NSF grant ARC-0804627 to Eberle. Samples from northeastern Siberia (Sib 13, DY 02, and DY 04) were collected by Schubert and W.M. Hagopian in 2013, with field support provided by N. Zimov, S. Zimov, and S.P. Davydov, logistical support by R.G.M. Spencer, E. Bulygina, and R.M. Holmes, and financial support by NSF grant EAR-1250063 to A.H. Jahren.

Appendix A. Supplementary data

Supplementary data to this article can be found online at <https://doi.org/10.1016/j.chemgeo.2023.121405>.

References

- Andreu-Hayles, L., Levesque, M., Martin-Benito, D., Huang, W., Harris, R., Oelkers, R., Leland, C., Martin-Fernández, J., Anchukaitis, K.J., Helle, G., 2019. A high yield cellulose extraction system for small whole wood samples and dual measurement of carbon and oxygen stable isotopes. *Chem. Geol.* 504, 53–65. <https://doi.org/10.1016/j.chemgeo.2018.09.007>.
- Baker, J.C.A., Gloor, M., Spracklen, D.V., Arnold, S.R., Tindall, J.C., Clerici, S.J., Leng, M. J., Brienen, R.J.W., 2016. What drives interannual variation in tree ring oxygen isotopes in the Amazon? *Geophys. Res. Lett.* 43 (22), 11831–11840. <https://doi.org/10.1002/2016GL071507>.
- Ballantyne, A.P., Rycyzynski, N., Baker, P.A., Harington, C.R., White, D., 2006. Pliocene Arctic temperature constraints from the growth rings and isotopic composition of fossil larch. *Palaeogeogr. Palaeoclimatol. Palaeoecol.* 242 (3), 188–200. <https://doi.org/10.1016/j.palaeo.2006.05.016>.
- Barbour, M.M., Andrews, T.J., Farquhar, G.D., 2001. Correlations between oxygen isotope ratios of wood constituents of Quercus and Pinus samples from around the world. *Funct. Plant Biol.* 28 (5), 335–348. <https://doi.org/10.1071/PP00083>.
- Borella, S., Leuenberger, M., Saurer, M., 1999. Analysis of $\delta^{18}\text{O}$ in tree rings: Wood-cellulose comparison and method dependent sensitivity. *J. Geophys. Res.-Atmos.* 104 (D16), 19267–19273. <https://doi.org/10.1029/1999JD900298>.
- Brendel, O., Iannetta, P., Stewart, D., 2000. A rapid and simple method to isolate pure alpha cellulose. *Phytochem. Anal.* 11 (1), 7–10. [https://doi.org/10.1002/\(SICI\)1099-1565\(200001/02\)11:1<7::AID-PCA488>3.0.CO;2-U](https://doi.org/10.1002/(SICI)1099-1565(200001/02)11:1<7::AID-PCA488>3.0.CO;2-U).
- Craig, H., 1954. Carbon 13 in Plants and the Relationships between Carbon 13 and Carbon 14 Variations in Nature. *J. Geol.* 62 (2), 115–149. <https://doi.org/10.1086/626141>.
- Csank, A.Z., Fortier, D., Leavitt, S.W., 2013. Annually resolved temperature reconstructions from a late Pliocene–early Pleistocene polar forest on Bylot Island, Canada. *Palaeogeogr. Palaeoclimatol. Palaeoecol.* 369, 313–322. <https://doi.org/10.1016/j.palaeo.2012.10.040>.
- Cullen, L.E., MacFarlane, C., 2005. Comparison of cellulose extraction methods for analysis of stable isotope ratios of carbon and oxygen in plant material. *Tree Physiol.* 25 (5), 563–569. <https://doi.org/10.1093/treephys/25.5.563>.
- Dansgaard, W., 1964. Stable isotopes in precipitation. *Tellus* 16 (4), 436–468. <https://doi.org/10.3402/tellusa.v16i4.8993>.
- Domínguez-Delmás, M., 2020. Seeing the forest for the trees: new approaches and challenges for dendroarchaeology in the 21st century. *Dendrochronologia* 62, 125731. <https://doi.org/10.1016/j.dendro.2020.125731>.
- Ferrio, J.P., Voltas, J., 2005. Carbon and oxygen isotope ratios in wood constituents of *Pinus halepensis* as indicators of precipitation, temperature and vapour pressure deficit. *Tellus Ser. B Chem. Phys. Meteorol.* 57 (2), 164–173. <https://doi.org/10.3402/tellusb.v57i2.16780>.
- Gaudinski, J.B., Dawson, T.E., Quideau, S., Schuur, E.A.G., Roden, J.S., Trumbore, S.E., Sandquist, D.R., Oh, S.-W., Wasylishen, R.E., 2005. Comparative analysis of cellulose preparation techniques for use with ^{13}C , ^{14}C , and ^{18}O isotopic measurements. *Anal. Chem.* 77 (22), 7212–7224. <https://doi.org/10.1021/ac050548u>.
- Gessler, A., Brandes, E., Buchmann, N., Helle, G., Rennenberg, H., Barnard, R., 2009. Tracing carbon and oxygen isotope signals from newly assimilated sugars in the leaves to the tree-ring archive. *Plant Cell Environ.* 32 (7), 780–795. <https://doi.org/10.1111/j.1365-3040.2009.01957.x>.
- Gessler, A., Ferrio, J.P., Hommel, R., Treydte, K., Werner, R.A., Monson, R.K., 2014. Stable isotopes in tree rings: towards a mechanistic understanding of isotope fractionation and mixing processes from the leaves to the wood. *Tree Physiol.* 34 (8), 796–818. <https://doi.org/10.1093/treephys/tpu040>.
- Gori, Y., Wehrens, R., Greule, M., Keppler, F., Ziller, L., La Porta, N., Camin, F., 2013. Carbon, hydrogen and oxygen stable isotope ratios of whole wood, cellulose and lignin methoxyl groups of *Picea abies* as climate proxies. *Rapid Commun. Mass Spectrom.* 27 (1), 265–275. <https://doi.org/10.1002/rcm.6446>.

- Gray, J., Thompson, P., 1977. Climatic information from 18O/16O analysis of cellulose, lignin and whole wood from tree rings. *Nature* 270 (5639), 708–709. <https://doi.org/10.1038/270708a0>.
- Green, J.W., 1963. Wood cellulose. *Methods Carbohydr. Chem.* 9–12.
- Greer, J.S., McInerney, F.A., Vann, D.R., Song, X., 2018. Evaluating methods for extraction of α -cellulose from leaves of *Melaleuca quinquenervia* for stable carbon and oxygen isotope analysis. *Rapid Commun. Mass Spectrom.* 32 (9), 711–720. <https://doi.org/10.1002/rcm.8085>.
- Guerrieri, R., Jennings, K., Belmecheri, S., Asbjornsen, H., Ollinger, S., 2017. Evaluating climate signal recorded in tree-ring $\delta^{13}\text{C}$ and $\delta^{18}\text{O}$ values from bulk wood and α -cellulose for six species across four sites in the northeastern US, 31 (24), 2081–2091. <https://doi.org/10.1002/rcm.7995>.
- Helle, G., Pauly, M., Heinrich, I., Schollan, K., Balanzategui, D., Schürbeck, L., 2022. Stable isotope signatures of wood, its constituents and methods of cellulose extraction. In: Siegwolf, R.T.W., Brooks, J.R., Roden, J., Saurer, M. (Eds.), *Stable Isotopes in Tree Rings: Inferring Physiological, Climatic and Environmental Responses*, 2022. Springer International Publishing, Cham, pp. 135–190. https://doi.org/10.1007/978-3-030-92698-4_5.
- Hook, B.A., Halfar, J., Bollmann, J., Gedalof, Z.E., Azizur Rahman, M., Reyes, J., Schulze, D.J., 2015. Extraction of α -cellulose from mummified wood for stable isotopic analysis. *Chem. Geol.* 405, 19–27. <https://doi.org/10.1016/j.chemgeo.2015.04.003>.
- Jahren, A.H., Sternberg, L.S.L., 2003. Humidity estimate for the middle Eocene Arctic rain forest. *Geology* 31 (5), 463–466. [https://doi.org/10.1130/0091-7613\(2003\)031<0463:HEFTME>2.0.CO;2](https://doi.org/10.1130/0091-7613(2003)031<0463:HEFTME>2.0.CO;2).
- Kagawa, A., Sano, M., Nakatsuka, T., Ikeda, T., Kubo, S., 2015. An optimized method for stable isotope analysis of tree rings by extracting cellulose directly from cross-sectional laths. *Chem. Geol.* 393–394, 16–25. <https://doi.org/10.1016/j.chemgeo.2014.11.019>.
- Langenheim, J.H., 1990. *Plant Resins*. *Am. Sci.* 78 (1), 16–24.
- Leavitt, S.W., Danzer, S.R., 1993. Method for batch processing small wood samples to holocellulose for stable-carbon isotope analysis. *Anal. Chem.* 65 (1), 87–89. <https://doi.org/10.1021/ac00049a017>.
- Li, Z.-H., Labbé, N., Driese, S.G., Grissino-Mayer, H.D., 2011. Micro-scale analysis of tree-ring $\delta^{18}\text{O}$ and $\delta^{13}\text{C}$ on α -cellulose spline reveals high-resolution intra-annual climate variability and tropical cyclone activity. *Chem. Geol.* 284 (1–2), 138–147. <https://doi.org/10.1016/j.chemgeo.2011.02.015>.
- Loader, N.J., Street-Perrott, F.A., Daley, T.J., Hughes, P.D.M., Kimak, A., Levanić, T., Mallon, G., Mauquoy, D., Robertson, I., Roland, T.P., van Bellen, S., Ziehmer, M.M., Leuenberger, M., 2015. Simultaneous determination of stable carbon, oxygen, and hydrogen isotopes in cellulose. *Anal. Chem.* 87 (1), 376–380. <https://doi.org/10.1021/ac502557x>.
- Lukens, W.E., Eze, P., Schubert, B.A., 2019. The effect of diagenesis on carbon isotope values of fossil wood. *Geology* 47 (10), 987–991. <https://doi.org/10.1029/2019JD03051210.1130/g46412.1>.
- Managave, S., Shimla, P., Yadav, R.R., Ramesh, R., Balakrishnan, S., 2020. Contrasting centennial-scale climate variability in High Mountain Asia revealed by a tree-ring oxygen isotope record from Lahaul-Spiti. *Geophys. Res. Lett.* 47 (4), e2019GL086170. <https://doi.org/10.1029/2019GL086170>.
- McCarroll, D., Loader, N.J., 2004. Stable isotopes in tree rings. *Quat. Sci. Rev.* 23 (7), 771–801. <https://doi.org/10.1016/j.quascirev.2003.06.017>.
- Miranda, J.C., Lehmann, M.M., Saurer, M., Altman, J., Treydte, K., 2021. Insight into Canary Island pine physiology provided by stable isotope patterns of water and plant tissues along an altitudinal gradient. *Tree Physiol.* 41 (9), 1611–1626. <https://doi.org/10.1093/treephys/tpab046>.
- Müller, K., 2020. Here: A Simpler Way to Find Your Files R package version 1.0.1. <https://CRAN.R-project.org/package=here>.
- Nakai, W., Okada, N., Sano, M., Nakatsuka, T., 2018. Sample preparation of ring-less tropical trees for $\delta^{13}\text{C}$ measurement in isotope dendrochronology. *Tropics* 27 (2), 49–58. <https://doi.org/10.3759/tropics.MS17-09>.
- Nissenbaum, A., Yakir, D., Langenheim, J.H., 2005. Bulk carbon, oxygen, and hydrogen stable isotope composition of recent resins from amber-producing Hymenaea. *Naturwissenschaften* 92 (1), 26–29. <https://doi.org/10.1007/s00114-004-0580-2>.
- Pons, T.L., Helle, G., 2011. Identification of anatomically non-distinct annual rings in tropical trees using stable isotopes. *Trees* 25 (1), 83–93. <https://doi.org/10.1007/s00468-010-0527-5>.
- Rees-Owen, R.L., Newton, R.J., Ivanovic, R.F., Francis, J.E., Riding, J.B., Marca, A.D., 2021. A calibration of cellulose isotopes in modern prostrate *Nothofagus* and its application to fossil material from Antarctica. *Sci. Total Environ.* 754, 142247. <https://doi.org/10.1016/j.scitotenv.2020.142247>.
- Ren, J., Schubert, B.A., Lukens, W.E., Quan, C., 2021. Low oxygen isotope values of fossil cellulose indicate an intense monsoon in East Asia during the late Oligocene. *Palaeogeogr. Palaeoclimatol. Palaeoecol.* 577, 110556. <https://doi.org/10.1016/j.palaeo.2021.110556>.
- R Core Team, 2022. *RStudio: v. 4.2.2*.
- Richter, S.L., Johnson, A.H., Dranoff, M.M., LePage, B.A., Williams, C.J., 2008a. Oxygen isotope ratios in fossil wood cellulose: isotopic composition of Eocene- to Holocene-aged cellulose. *Geochim. Cosmochim. Acta* 72 (12), 2744–2753. <https://doi.org/10.1016/j.gca.2008.01.031>.
- Richter, S.L., Johnson, A.H., Dranoff, M.M., Taylor, K.D., 2008b. Continental-scale patterns in modern wood cellulose $\delta^{18}\text{O}$: implications for interpreting paleo-wood cellulose $\delta^{18}\text{O}$. *Geochim. Cosmochim. Acta* 72 (12), 2735–2743. <https://doi.org/10.1016/j.gca.2008.01.030>.
- Roden, J.S., Lin, G., Ehleringer, J.R., 2000. A mechanistic model for interpretation of hydrogen and oxygen isotope ratios in tree-ring cellulose. *Geochim. Cosmochim. Acta* 64 (1), 21–35. [https://doi.org/10.1016/S0016-7037\(99\)00195-7](https://doi.org/10.1016/S0016-7037(99)00195-7).
- Sauer, P.E., Sternberg, L.D.S.L.O., 1994. Improved method for the determination of the oxygen isotopic composition of cellulose. *Anal. Chem.* 66 (14), 2409–2411. <https://doi.org/10.1021/ac00086a030>.
- Schubert, B.A., Jahren, A.H., 2015. Seasonal temperature and precipitation recorded in the intra-annual oxygen isotope pattern of meteoric water and tree-ring cellulose. *Quat. Sci. Rev.* 125, 1–14. <https://doi.org/10.1016/j.quascirev.2015.07.024>.
- Schubert, B.A., Jahren, A.H., Davydov, S.P., Warny, S., 2017. The transitional climate of the late Miocene Arctic: winter-dominated precipitation with high seasonal variability. *Geology* 45 (5), 447–450. <https://doi.org/10.1130/g38746.1>.
- Sidorova, O.V., Siegwolf, R.T.W., Saurer, M., Naurzbaev, M.M., Shashkin, A.V., Vaganov, E.A., 2010. Spatial patterns of climatic changes in the Eurasian north reflected in Siberian larch tree-ring parameters and stable isotopes. *Glob. Chang. Biol.* 16 (3), 1003–1018. <https://doi.org/10.1111/j.1365-2486.2009.02008.x>.
- Song, X., Lorrey, A., Barbour, M.M., 2022. Environmental, physiological and biochemical processes determining the oxygen isotope ratio of tree-ring cellulose. In: Siegwolf, R.T.W., Brooks, J.R., Roden, J., Saurer, M. (Eds.), *Stable Isotopes in Tree Rings: Inferring Physiological, Climatic and Environmental Responses*, 2022. Springer International Publishing, Cham, pp. 311–329. https://doi.org/10.1007/978-3-030-92698-4_10.
- Sternberg, L.D.S.L., Pinzon, M.C., Vendramini, P.F., Anderson, W.T., Jahren, A.H., Beuning, K., 2007. Oxygen isotope ratios of cellulose-derived phenylglucosazone: An improved paleoclimate indicator of environmental water and relative humidity. *Geochim. Cosmochim. Acta* 71 (10), 2463–2473. <https://doi.org/10.1016/j.gca.2007.03.004>.
- Szymczak, S., Joachimski, M.M., Bräuning, A., Hetzer, T., Kuhlemann, J., 2011. Comparison of whole wood and cellulose carbon and oxygen isotope series from *Pinus nigra* ssp. *laricio* (Corsica/France). *Dendrochronologia* 29 (4), 219–226. <https://doi.org/10.1016/j.dendro.2011.04.001>.
- Tiedemann, F., 2022. gghalves: Compose Half-Half Plots Using Your Favourite Geoms R package version 0.1.4. <https://CRAN.R-project.org/package=gghalves>.
- Volts, J., Chambel, M.R., Prada, M.A., Ferrio, J.P., 2008. Climate-related variability in carbon and oxygen stable isotopes among populations of Aleppo pine growth in common-garden tests. *Trees* 22 (6), 759–769. <https://doi.org/10.1007/s00468-008-0236-5>.
- Vornlocher, J.R., Lukens, W.E., Schubert, B.A., Quan, C., 2021. Late Oligocene Precipitation Seasonality in East Asia based on $\delta^{13}\text{C}$ Profiles in Fossil Wood. *Palaeogeogr. Palaeoclimatol.* 36 (4), e2021PA004229. <https://doi.org/10.1029/2021PA004229>.
- Westerhold, T., Marwan, N., Drury, A.J., Liebrand, D., Agnini, C., Anagnostou, E., Barnett, J.S.K., Bohaty, S.M., De Vleeschouwer, D., Florindo, F., Frederichs, T., Hodell, D.A., Holbourn, A.E., Kroon, D., Laurentino, V., Littler, K., Lourens, L.J., Lyle, M., Pälike, H., Röhl, U., Tian, J., Wilkens, R.H., Wilson, P.A., Zachos, J.C., 2020. An astronomically dated record of Earth's climate and its predictability over the last 66 million years. *Science* 369 (6509), 1383–1387. <https://doi.org/10.1029/2019JD03051210.1126/science.aba6853>.
- Wickham, H., Averick, M., Bryan, J., Chang, W., McGowan, L., François, R., Grolemund, G., Hayes, A., Henry, L., Hester, J., 2019. Welcome to the tidyverse, 4 (43), 1686. <https://doi.org/10.21105/joss.01686>.
- Wieloch, T., Helle, G., Heinrich, I., Voigt, M., Schyma, P., 2011. A novel device for batch-wise isolation of α -cellulose from small-amount wholewood samples. *Dendrochronologia* 29 (2), 115–117. <https://doi.org/10.1016/j.dendro.2010.08.008>.
- Wright, W.E., 2008. Statistical evidence for exchange of oxygen isotopes in holocellulose during long-term storage. *Chem. Geol.* 252 (1), 102–108. <https://doi.org/10.1016/j.chemgeo.2008.01.016>.
- Xu, C., Sano, M., Nakatsuka, T., 2011. Tree ring cellulose $\delta^{18}\text{O}$ of *Fokienia hodginsii* in northern Laos: a promising proxy to reconstruct ENSO? *J. Geophys. Res.-Atmos.* 116 (D24). <https://doi.org/10.1029/2011JD016694>.
- Xu, C., Sano, M., Dimri, A.P., Ramesh, R., Nakatsuka, T., Shi, F., Guo, Z., 2018. Decreasing Indian summer monsoon on the northern Indian sub-continent during the last 180 years: evidence from five tree-ring cellulose oxygen isotope chronologies. *Clim. Past* 14 (5), 653–664. <https://doi.org/10.5194/cp-14-653-2018>.
- Xu, C., Zhao, Q., An, W., Wang, S., Tan, N., Sano, M., Nakatsuka, T., Borhara, K., Guo, Z., 2021. Tree-ring oxygen isotope across monsoon Asia: common signal and local influence. *Quat. Sci. Rev.* 269, 107156. <https://doi.org/10.1016/j.quascirev.2021.107156>.
- Zech, M., Mayr, C., Tuthorn, M., Leiber-Sauheitl, K., Glaser, B., 2014. Oxygen isotope ratios ($^{18}\text{O}/^{16}\text{O}$) of hemicellulose-derived sugar biomarkers in plants, soils and sediments as paleoclimate proxy I: Insight from a climate chamber experiment. *Geochim. Cosmochim. Acta* 126, 614–623. <https://doi.org/10.1016/j.gca.2013.10.048>.